$16^{èmes}$ Journées Internationales de Thermique (JITH 2013)
Marrakech (Maroc), du 13 au 15 Novembre, 2013

SIMULATION OF A CONFINED LAMINAR DIFFUSION METHANE JET FLAME: COMPARISON OF TWO CHEMICAL KINETICS MECHANISMS

Ahmed GUESSAB[1], Abdelkader ARIS[2], Tawfik Benabdellah[3], Mourad TAHAJANAN[4]

[1, 3]Industrial Products and Systems Innovations Laboratory (IPSILab), ENP Oran, Algeria
[2]LCGE, USTOMB, Oran, Algeria.
[4]Laboratoire de Mécanique des Fluides, ENSET de Rabat, Maroc.
*(E-mail : **med_guessab@yahoo.fr**)*

Abstract: Two chemical kinetic mechanisms of methane combustion were tested and compared using a confined axisymmetric laminar flame: 1-step global reaction mechanism (Westbrook and Dryer, 1981) and 4-step mechanism (Jones and Lindstedt, 1988) to predict the velocity, temperature and species distributions that describe the Finite rate chemistry of methane combustion. The transport equations are solved by FLUENT using a finite-volume method with a SIMPLE procedure. The numerical results are presented and compared with the experimental data (Xu and Smook, 1993) [1]. A 4-step methane mechanism was successfully implanted into CFD solver Fluent. The precompiled mechanism was linked to the solver by the means of a User Defined Function (UDF). The numerical solution is in very good agreement with previous numerical of 4-step mechanism and the experimental data.

Keywords: Diffusion Flame, Laminar , Co-flow, UDF, Chemical kinetic, Finite Rate Chemistry .

1. Problem Description

In summary, the major works of present paper include comparison between 1-step and 4-step chemical reaction mechanism. A working model was developed that fully coupled a comprehensive chemical kinetic mechanism with computational fluid dynamics in the commercial software program Fluent modified such as to deal with Westbrook's and Drayer, [2], Jones *et al*. [3]. The vertical cylindrical diffusion flame burner is shown in Figure 1. The burner consists of two concentric tubes of 12.7 mm and 50.8 mm. Fuel issues through the inner tube and air issues through the outer. The fuel-jet velocity is 0.0455 m/s, with a temperature of 300K. A uniform velocity 0.0988 m/s is specified for the air coflow with a temperature of 300K. The methane-jet is supplied at 3.71×10^{-6} Kg/s, or the Air is supplied at 2.214×10^{-4} Kg/s. The exit pressure is specified 10^5 Pa, whereas a zero-gradient pressure conditions is imposed at the inlet. The wall-function treatment is utilized at the walls. The fuel-jet and air co-flow compositions are specified in terms of the species mass fraction and based on the information provided about the experiment [1]. In the present computation, the reaction rate is computed by finite-rate for laminar flow. The 1-step and 4-step reactions are used in methane combustion (Tables 1and 2).

Table 1: Westbrook and Dryer Global Multi-Step Chemical Kinetics Mechanism for CH_4/air combustion and reaction rate coefficients [2].

No.	**Reaction**	A_k	β_k	E_k *[j/molK]*	**Reaction orders**
WD1	$CH_4+2O_2 \rightarrow CO_2+2H_2O$	1.0e+12	0	1.0e+08	$[CH4]^{0.5}\,[O2]^{1.25}$

Table 2: Jones Lindstedt Global Multi-Step Chemical Kinetics Mechanism for CH_4/air combustion and reaction rate coefficients [3].

No.	**reaction**	A_k	β_k	E_k *[Kj/mol]*	**Reaction orders**
JL1	$CH_4+0.5O_2 \rightarrow CO+2H_2$	7.82e+13	0	30.0e+03	$[CH_4]^{0.5}\,[O_2]^{1.25}$
JL2	$CH_4+H_2O \rightarrow CO+3H_2$	0.30e+12	0	30.0e+03	$[CH_4][H_2O]$
JL3	$H_2+0.5O_2 \rightarrow H_2O$	1.21e+18	-1	40.0e+03	$[H_2]^{0.25}[O_2]^{1.5}$
JL4	$CO+H_2O \rightarrow CO_2+H_2$	2.75e+12	0	20.0e+03	$[CO][H_2O]$

2. Governing equations

The description of a problem in combustion can be given by the conservation equation of mass, momentum, species concentrations and energy. The finite rate model of all reactions mechanisms can be written as follows:

2.1. The laminar finite rate model

$$\hat{R}_i = M_{w,i} \sum_{k=1}^{N_R} \hat{R}_{i,k} \qquad (1)$$

2.2. The Arrhenius Rate

In general, a chemical reaction can be written in the form as follows:

$$\sum_{i=1}^{N} \upsilon'_{i,k} A_i \Leftrightarrow \sum_{i'=1}^{N} \upsilon''_{i,k} A_i \qquad (2)$$

Where

N = number of chemical species in the system
$\upsilon'_{i',k}$ = Stoichiometric coefficient for reactant i in reaction k
$\upsilon''_{i',k}$ = Stoichiometric coefficient for product i in reaction k
A_i = chemical symbol denoting species i
$k_{f,k}$ = forward rate constant for reaction k
$k_{b,k}$ = backward rate constant for reaction k

Equation (2) is valid for both reversible and non-reversible reactions. For non-reversible reactions, the backward rate constant $k_{b,k}$ is simply omitted. The summations in Equation (2) are for all chemical species in the system, but only species involved as reactants or products will have non-zero stoichiometric coefficients, species that are not involved will drop of the equation except for third-body reaction species. The molar rate of creation/destruction of species *i'* in reaction *k*, $\hat{R}_{i',k}$, in Equation (1) $\hat{R}_{i',k}$ is given by:

$$\hat{R}_{i',k} = \Gamma\left(\upsilon''_{i,k} - \upsilon'_{,k}\right)\left(k_{f,k} \prod_{j=1}^{N} \left[C_j\right]^{\eta'_{j,k}} - k_{b,k} \prod_{j=1}^{N} \left[C_j\right]^{\eta''_{j,k}}\right) \qquad (3)$$

Where:

C_j = Molar concentration of each reactant or product species j [Kmol m^{-3}]
$\eta_{j,k}$ = Rate exponent for reactant *j'* in reaction *k*
η'_{jk} = Rate exponent for product *j'* in reaction *k*
Γ = represents the net effect of third bodies on the reaction rate. This term is given by:

$$\Gamma = \sum_{j'}^{N} \gamma_{j,k} C_j \qquad (4)$$

Where $\gamma_{j'k}$ is the third-body efficiency of the $j'th$ species in the *k*th reaction. The forward rate constant for reaction k, $k_{f,k}$, is computed using the Arrhenius expression

$$k_{f,k} = A_k T^{\beta_k} \exp\left(-E_k/RT\right) \qquad (5)$$

Where:

A_k = pre-exponential factor (consistent units)
β_k = temperature exponent (dimensionless)
E_k = activation energy for the reaction [J Kgmol^{-1}]
R = universal gas constant [J Kmol^{-1}K^{-1}]

The values of $\upsilon'_{i,k}, \upsilon''_{',k}, \eta'_{',k}, \eta''_{i,k}, \beta_k, A_k, E_k$ and $\gamma_{j'k}$ can be provided the problem definition. If the reaction is reversible, the backward rate constant for reaction *k*, $k_{b,k}$, is computed from the forward rate constant using the following relation:

$$k_{b,k} = \frac{k_{f,k}}{K_k} \qquad (6)$$

Where k_k is the equilibrium constant for the *k*-th reaction. Computed from:

$$K_k = \exp\left(\frac{\Delta S_k^0}{R} - \frac{\Delta H_k^0}{RT}\right)\left(\frac{P_{atm}}{RT}\right)^{\sum_{k=1}^{NR}\left(\upsilon''_{i,k} - \upsilon'_{i,k}\right)} \qquad (7)$$

Where P_{atm} denotes atmospheric pressure (101325Pa). The term within the exponential represents the change in Gibbs free energy, and its components are computed as follows:

$$\frac{\Delta S_k{}^{\circ}}{R} = \sum_{i'=1}^{N} \left(\upsilon''_{i,k} - \upsilon'_{i,k}\right) \frac{S_i^0}{R} \quad ; \quad \frac{\Delta H_k^0}{RT} = \sum_{i'=1}^{N} \left(\upsilon''_{i,k} - \upsilon'_{i,k}\right) \frac{h_i^0}{R} \qquad (8), (9)$$

Where $S_{i'}^0$ and $h_{i'}^0$ are, respectively, the standard-state entropy and standard-state enthalpy including heat of formation.

3. Simulation Details

The governing equations are solved using the CFD package Fluent [4] modified with User Defined Functions (UDF) in order to integrate the reaction rate formula proposed by Westbrook *et al*. [2] and Jones *et al*. [3]. We have used Finite-Rate approach. In CFD, the differential equations govern the problem are discretized into finite volume and then solved using algebraic approximations of differential equations. These numerical approximations of the solution are then iterated until adequate flow convergence is reached. The chemical kinetics information is then coupled into fluid dynamics equations to allow both phenomena to be incorporate into a single problem. The SMPLE algorithm [4] of velocity-coupling was used in which the mass conservation solution is used to obtain the pressure field at each flow iteration. The numerical approximations for momentum, energy, and species transport equations were all set to first order upwind. This means that the solution approximation in each finite volume was assumed to be linear. This saved on computational expense. In order to properly justify using a first order scheme, it was necessary to show that the grid used in this work had adequate resolution to accurately capture the physics occurring within the domain. In other words, the results needed to be independent of the grid resolution. This was verified by running simulations with higher resolution grids. In a reacting flow such as that studied in this work, there are significant time scale differences between the general flow characteristics and the chemical reactions. In order to handle the numerical difficulties that arise from this, the STIFF Chemistry Solver was enabled in Fluent. For more information about this technique refer to Fluent [4]. Overall, the computational model solved the following flow equations: mass continuity, *r* momentum, *x* momentum, energy, and *n-1* species conservation equations where *n* is the number of species in the reaction. The *n-th* species was determined by the simple fact that the summation of mass fractions in the system must equal one. The combustion system, the vertical, cylindrical diffusion flame burner [1] as can be seen in Figure 1, consists of two concentric tubes through which the fuel and air issue, respectively. The burner nozzle was set as inlet with a uniform velocity normal to the boundary. The exhaust of the burner was set as an atmospheric pressure outlet. The walls were set as adiabatic with zero flux of both mass and chemical species. Due to the geometry of the model, only half of the domain needed to be modeled since a symmetry condition could be assumed along the centerline of the burner. The boundary conditions, following Xu and Smoot [1], it was assumed that the combustion chamber walls were maintained at the temperature of 300K, in addition to the non-slip and impermeability conditions. The wall roughness constants and roughness height are the default values provided by Fluent (0 m and 0.5 m, respectively). In the symmetry axis, it was considered that the axial velocity gradient in the radial direction is null. The outlet condition for all variables was null diffusive flux. The axial velocity component, after the outlet of chamber, was corrected by a factor to conserve the mass and avoid counter-flow. In the entire chamber outlet plane the radial velocity component was set null. The wall emissivities were equal to 0.6. The inlet and outlet reservoirs were represented as black surfaces at the temperature of the inlet and outlet gases, respectively. The outlet temperature was computed as $\overline{T}_{bulk} = \left(r\bar{u}C_P\overline{T}\right)/\left(r\bar{u}C_p\right)$ where $\overline{T}_{bulk}$ was the average temperature of the mixture in the outlet. In the inlet, the flow velocity in the axial direction and the concentration profiles were assumed uniform. The turbulent kinetic energy was taken as $k = \frac{3}{2}\left(\bar{u}_{in} I_{turb}\right)^2$ (given by Fluent Inc. [4]), where I_{turb} is the turbulence intensity given by $I_{turb} = \frac{U'_{rms}}{\overline{U}} = \frac{0.16}{\left(Re_H\right)^{1/8}}$ [4] and u_{in} is the inlet axial velocity. For the destruction of the turbulent kinetic energy, it was specified $\varepsilon = C_\mu^{3/2} k^{3/2} / l$ of the turbulence scale, where C_μ= 0.09 is an empirical constant and *l* [m] is the turbulence length scale estimated from $l = 0.07D_H$ [4], where D_H [m] is the hydraulic diameter. This approach to estimation of k and ε at the inlet assumes fully developed flow. The turbulence intensity at the inlet was prescribed as 1 % for the air and 6.5 % for the fuel. For the dissipation of the turbulent kinetic energy, it was employed a characteristic length of 1mm for the air and 0.57mm for the fuel. In the region close to the wall, it was also applied a mesh refinement to capture the boundary layer effects. The constant pressure specific heat capacity C_p for the gas mixture is determined from ($C_P = \sum_{1}^{N} Y_i C_{P,i}$) as the sum of the mass fraction weighted C_p of each species. C_{pi} is determined from the polynomial functions of temperature. The default polynomials provided in FLUENT are used. The C_p polynomial provided for CH_4 is used for the numerical fuel. As the natural gas is primarily comprised of CH_4 the error introduced by using the C_p of CH_4 for the entire hydrocarbon fraction of the natural gas is assumed to be minimal. The criterion of convergence is the summation of residual mass sources less than 10^{-5} for the other terms of the transport equations and is 10^{-8} for energy equation. The measured width of the jet is always small compared to the width of the channel so the pattern is not directly influenced by partial effects (containment viscous interaction, etc...). This allows us to assume that the jet is axisymmetric and use two-dimensional approach to simplify the calculation. The computational space seen in Figure 1 given a finite volume mesh is divided by a staggered non-uniform quadrilateral cell (Figure 2). The computational domain extends for 0.3 m after the burner nozzle, and 0.00508 m from the centerline. These dimensions correspond to $48d_{jet}$ and $0.8d_{jet,}$ respectively. A total number of 1500 (50×30) quadrilateral cells were generated using non-uniform grid spacing to provide an adequate resolution near the jet axis and close to the burner where gradients were large.

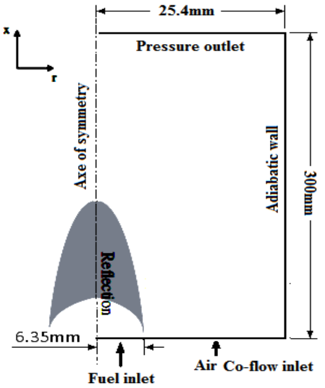

Figure 1: Geometry of confined axisymmetric laminar diffusion flame [1].

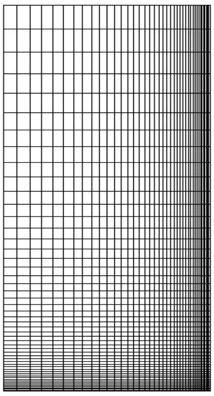

Figure 2 : Grid

4. Results

In this study, the 4-step reduced mechanism has been implemented and tested in Fluent. Fluent has UDF capabilities to allow for such implementation. The precompiled mechanism was linked to the solver by the means of a User Defined Function (UDF). The UDF communicates the chemical source terms the solver through the subroutine 'Define Net Reaction Rates'. The subroutine then returns the molar production rates of the species given the pressure, temperature, and mass fractions. We begin by comparing the computational cost of the two kinetic models in terms of the average CPU (execution) time per time step. The relative elapsed CPU times are compared in Table 3. In the 4-step mechanism [3], more reaction equations are computed, them more CPU time is spent and more difficult it is to convergence. Figure 3 shows the contour plot of the temperature for temperature fields from the simulation using the 'WD' and 'JL' mechanism (Figure 3b and 3c) compared with experiment [1] (Figure 3a). Is noticed that the smallest flame is predicted by the 1-step model 'WD', whereas the largest flame is predicted by the 4-step model 'JL' (Figure 3c) and it is observed that the predicted maximum temperature calculated for the laminar co-flow diffusion flame using different chemical kinetic schemes for 1-step model is 2218 K, but in the 4-step scheme, it is 1955 K. The maximum center-line temperature reported by Xu *et al.* is 2180 K. The 1-step mechanism assumes that the reaction products are CO_2 and H_2O, the total heat of reaction is over predicted. In the actual situation, some CO and H_2 exist in the combustion products with CO_2 and H_2O. This lowers the total heat of reaction and decreases the flame temperature. The 4-step mechanism includes CO and H_2, so we can get more detailed chemical species distribution.

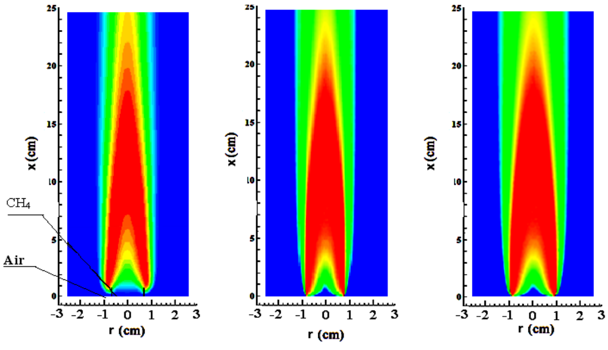

Xu *et al.* [1]
(a)

Predicted 1-step (WD)
(b)

Predicted 4-step (JL)
(c)

Figure 3: Shape and size of the flame CH_4/Air.

Table 3: Average execution time per time step.

Kinetic model	1-step [WD]	4-step [JL]
Species	5	6
Reactions	1	4
CPU Time/iteration (s)	0.00396	0.0554
Nb. iterartions	635	2845

The radial profiles of axial velocity for two axial locations (x=1.2 and 5 cm) are shown in figure 4. The agreement between the prediction and measurement is very good. The axial velocity away from the centerline decreases at all heights and becomes very low beyond a radial distance. Radial composition profiles of CH_4, O_2, CO_2 and H_2O at x=1.2 cm are shown on Figure 5 and the test results for Xu *et al.* [1] are also shown. The comparison of CO and H_2 is shown in Figure 6 and 7. In general, the numerical solution is in very good agreement with previous numerical of 4-step reduced mechanism and the experimental data.

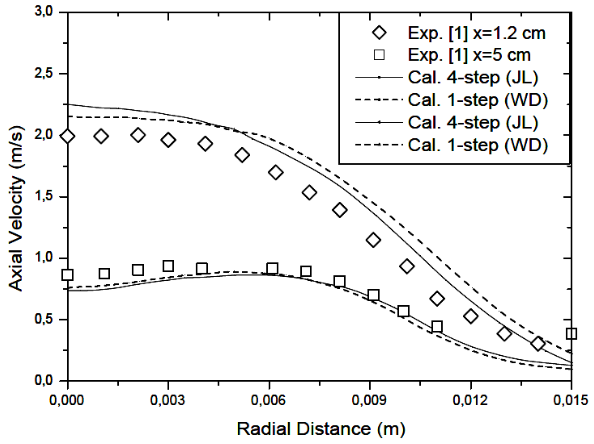

Figure 4: Radial profiles of axial velocity.

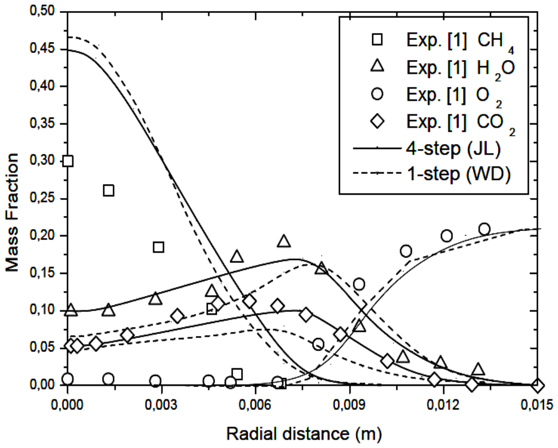

Figure 5: Radial profiles of the species mass fractions at x=1.2cm.

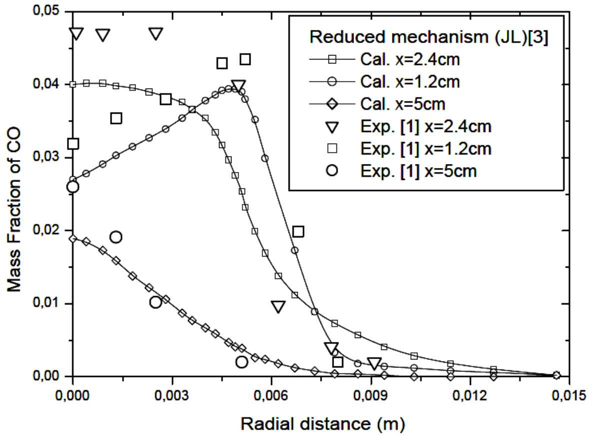

Figure 6: Radial CO mole fraction profiles.

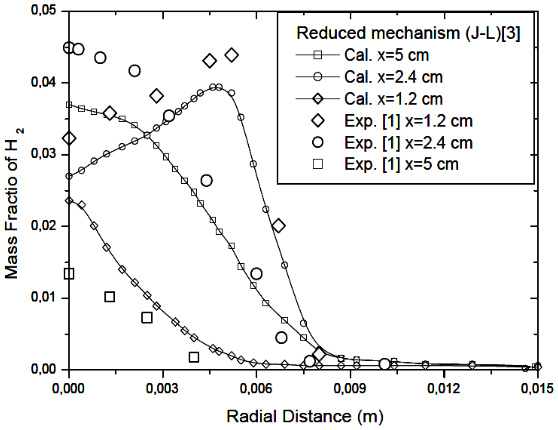

Figure 7: Radial H_2 mole fraction profiles.

5. Conclusion

This study constitutes the initial steps in the development of an efficient numerical scheme for the simulation of unsteady, multidimensional combustion with stiff detailed chemistry. The following conclusions were obtained:

- The 7 species global mechanism was successfully implemented and tested into the CFD solver FLUENT.
- The precompiled mechanism was linked to the solver by the means of a User Defined Function (UDF) which communicates the chemical source terms to the solver through the subroutine “Define Net Reaction Rates” and the Implementation of the UDF was tested with the Xu *et al.* CH_4/Air laminar flame.

References

[1] Xu, Y., Smooke, M.D., Lin, P. and Long, M.B., Primitive Variable Modeling of Multidimensional Laminar Flames. Combustion Science and Technology, 90, 289-313, (1993).

[2] Westbrook, C. K., Dryer, F. L., Simplified Reaction Mechanisms for the Oxidation of Hydrocarbon Fuels in Flames, Combustion Sciences and Technologies, 27(1981), 1-2, pp. 31-43.

[3] Jones W. P., and Lindstedt R. P., *Combustion and Flame* 73, 233 – 249 (1988).

[4] FLUENT. 2010. “Theory Guide: Release 12.0.” Last modified January 23, (2009).